A Simple Experimental Method Based on Linear Near-Field Measurements to calculate the Phase Center of an Antenna

Enrique G. Plaza, G. León, S. Loredo, L. F. Herrán,
Area of Signal Theory and Communications, Universidad de Oviedo, Gijón, Spain,
{ egplaza, gleon, sloredo, lfherran }@tsc.uniovi.es

***Abstract*—In this paper, a simple experimental method based on linear Near-Field measurements for finding the real position of the phase center of an antenna is presented. In order to do that, measurements along both principal axes of the antenna are carried out. Then, each set of data is treated individually to determine the phase center for each principal plane. In this method, the measured phase is expressed in terms of the relative position to the axis as a quadratic expression, in which the independent term gives the perpendicular distance from the points of the measurement to the estimated phase center. Thus, this value is obtained by adjusting a second-order polynomial expression to the curve of the measured phased. The operational limits of the method are generally determined by the amplitude variation of the measured field. In order to establish these limits and verify its functionality, a series of simulations have been carried out. Finally, the method has been used to characterize some real antennas.**

***Keywords*—** Phase center, horn antenna, antenna characterization, Near-Field

I. Introduction

The Phase Center (PhC) of an antenna is, by definition, the point where its phase front is originated. Typically, it is assumed to be placed at the central point of its aperture. Although this approximation might be adequate for a Far-Field (FF) analysis of the antenna, it may not be accurate enough for other applications. For instance, when the antenna is used to feed a reflectarray [1] or transmitarray [2], the PhC should be placed at the focus of the system in order to optimize its behavior. Therefore, it is previously necessary to determine the PhC position in order to complete the required characterization of the feed.

Many different models have been proposed to fulfill this task [3]-[6]. In [3], Padilla et alter proposed two different methods to determine the PhC position of a rod antenna that can be applied to any other case. In the first one, the PhC is assumed to be displaced an unknown distance in the Z-Axis (Δ_z) which is calculated by minimizing, using the least square method, the difference between the measured phase and the theoretical one obtained by assuming that displacement of the PhC. The second method consists on directly finding the PhC by moving the antenna alongside the perpendicular axis while it is feeding a parabolic reflector. Given that the focus of the system is known, the PhC of the antenna is obtained when a planar phase-front is measured, since, in that case, the Antenna Under Test (AUT) would be placed at the focus of the structure. In [4], a method similar to the first one is presented, but in this case the PhC might be displaced in the three axes (Δ_x,Δ_y,Δ_z) since the measurement takes place in an anechoic chamber. Although all these methods are based on the study of the measured phase, it is also possible to carry out an analysis based on the theoretical study of the structure [5] or the amplitude of the measured field [6]. In this case, Costa et alter [6] determine the PhC of a dielectric lens under test by using two antennas to feed another dielectric lens, the one under test and a second one which is fully characterized. Thus, by comparing the maxima of both measured amplitudes, the difference between them gives the distance between both PhCs and therefore, the position of the PhC of the dielectric lens under test.

The objective of the method proposed in this paper is to reduce the number of points required in the analysis and its complexity in comparison to those which use the measured phase. This simple experimental method is based on the fact that the distance from the PhC to the points of one of the principal axes can be expressed as a function of the measured phase as well as of the coordinates of all the points at which the field is acquired. Thus, it is possible to adjust the measured phase with a quadratic polynomial in which the perpendicular distance to the PhC is given by the independent term of the expression. This method presents a good and stable behavior as long as the measure is kept within certain working limits. In order to prove the functionality of the method, it has been tested with a series of simulations. Afterwards, it has been used to characterize some antennas by measuring them in a near-field planar range.

II. Method

A. Centered case

The working principle of the model proposed in this paper consists in measuring the Near-Field (NF) of the AUT at a distance (Z_1) from its aperture (see Fig. 1), and then, by using the measured phase, being able to obtain the perpendicular distance from the points of the measurement to the PhC (z_0). Hence, assuming a measurement along the X-Axis, the distance from the measurement points to the PhC on Cartesian coordinates can be written as:

$$d^2 = (x - x_0)^2 + y_0^2 + z_0^2, \tag{1}$$

where (x_0, y_0, z_0) is the unknown position, see Figs. 1(a) and 1(b), of the PhC in relation to the central point of the measurements. Nonetheless, if the AUT is centered in relation to Y-axis of the measurement system ($y_0 = 0$) , it can be assumed that the PhC is located along the axis where the data are acquired. Thus, (1) transforms into:

$$d^2 = x^2 - 2xx_0 + x_0^2 + z_0^2. \tag{2}$$

On the other hand, the term x_0 cannot be left out of the equation. Nevertheless, it can be assumed that x_0 tends to 0. Therefore, the value of x_0^2 would be negligible in comparison to the rest of the terms. This way, (2) can be expressed as the following quadratic polynomial:

$$d^2 = x^2 - 2x_0x + z_0^2. \tag{3}$$

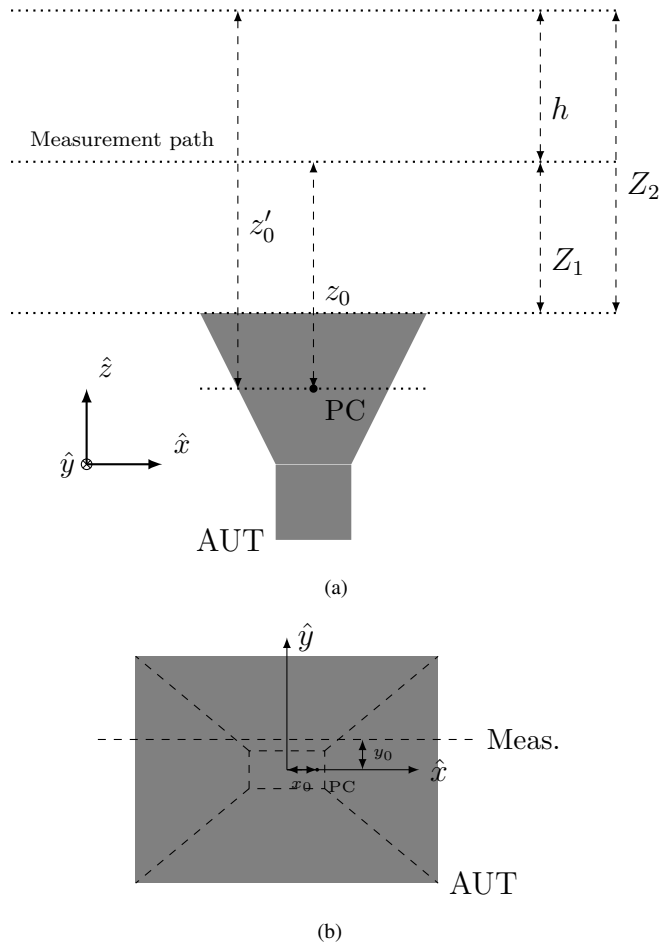

Fig. 1. Scheme of the method working principle.

In addition, the distance can also be written in terms of the measured phase, based on the expression of the propagation term (e^{-jk_0d}). Thus, (4) and (5) are obtained, being k_0 the propagation constant and ϕ_{unw} the unwrapped values of the measured phase (ϕ_{meas}).

$$d^2 = \frac{\phi_{unw}^2}{k_0^2}, \tag{4}$$

$$\phi_{unw} = \phi_{meas} - 2n\pi, n \in \mathbb{N}, \tag{5}$$

And therefore, by relating (3) and (4), the following expression is obtained:

$$\frac{\phi_{unw}^2}{k_0^2} = Ax^2 - 2x_0x + z_0^2. \tag{6}$$

In this model, the left term of the expression is obtained directly from the measurements. The value of the parameter n is set in (5) to ensure that, when adjusting the measured data with a quadratic polynomial (6), the second order term (A) is as close to 1 as possible. All in all, since the value of n covers a wide interval, this feature would indicate the accuracy of the estimation. Furthermore, as it is seen in (6), the independent term would give the perpendicular distance (z_0) between the PhC and the points where the measurement was carried out and thus its relative position to the aperture of the AUT. If this process is to be repeated with another measurement, the difference between z_0' and z_0 has to be the same as the one between Z_1 and Z_2, that is h, as shown in Fig. 1. The lineal term would relate to the displacement of the PhC in the X-Axis, which usually has an almost negligible effect ($< 0.1\ mm$). If the measurements are taken along the Y-Axis, the role played by the parameters x_0 and y_0 is interchanged. Now, x_0 will be the displacement in the axis perpendicular to the measurement path and y_0 the PhC displacement along this Y-axis.

B. Displaced case

It may happen that, due to the geometry of the antenna or the positioning system, the PhC position is not aligned with the axis along which the measurement is carried out, and, as a result, y_0 has to be taken into account. This way, (6) is transformed into:

$$\frac{\phi_{unw}^2}{k_0^2} = x^2 - 2x_0x + (z_0^2 + y_0^2). \tag{7}$$

Then, in order to estimate the values of z_0 and y_0, it is necessary to carry out an additional measurement at a distance $Z_2 = Z_1 + h$, where the value of h is known (Fig. 1). Thus, by applying the method for both sets of measurements, two different independent terms, C_1 and C_2, are calculated:

$$C_1 = y_0^2 + z_0^2, \tag{8}$$

$$C_2 = y_0^2 + (z_0 + h)^2. \tag{9}$$

Finally by isolating z_0 and y_0 in (8) and (9), their values are obtained:

$$z_0 = \frac{C_2 - C_1 - h^2}{2h}, \tag{10}$$

$$y_0 = \sqrt{C_1 - z_0^2}. \tag{11}$$

In both cases, as long as the measurements are within the limits of use of the method, the results can be considered trustworthy. These limitations are usually related to the fitting of the phase curve which could include values of the field

not significant or secondary lobes. These features can add a certain error to the fitting polynomial and change the value of n used to fit the phase curve.

III. Simulations

The validation of the proposed method has been done by carrying out a series of simulations using FEKO v6.2 [7]. In each of the simulations, the PhC position is previously estimated by analyzing the field generated by the AUT at a certain distance from the aperture. In this study, the different antennas are going to be classified according to their directivity, which is one of the parameters that has a greater impact on the limits of the method, since the appearance of secondary lobes or the inclusion of non-significant elements can alter the results. Thus, three different antennas are studied, that is, one of low directivity, one of medium-high directivity and, finally, one with a very high directivity.

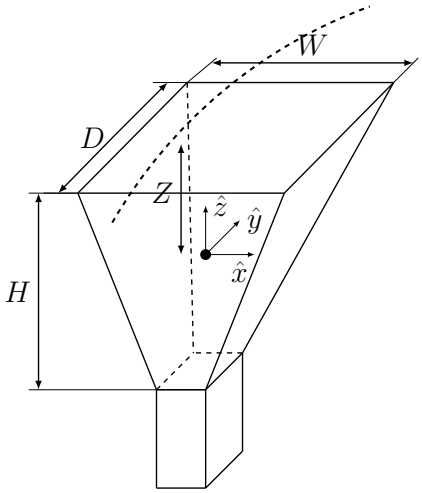

Fig. 2. Horn scheme.

A. Low directive antenna

The first AUT is a pyramidal horn antenna working at 18 GHz fed by a WR-42, whose dimensions are $H = 25$ mm, $W = 20$ mm and $D = 30$ mm (see Fig. 2). It presents a directivity of approximately 12 dBi. In Fig. 3, the phase of the electric field, acquired in a sphere, for the different cases according to its relative position (Z) to the aperture of antenna is depicted. It can be observed that both for X- and Y-axis the position of the PhC is approximately $Z = -2\ mm$.

The electric field has been acquired at several distances from the aperture of the antenna between -90 and 90 mm for axes X and Y and then the method was applied to the data. In Tables I and II it can be observed that the calculated position of the PhC, is approximately the same for all the distances at which the field has been acquired and it matches the one that had been previously estimated. This result serves as a validation for the method, since it is shown that it can provide a stable result for different sets of data using the same AUT.

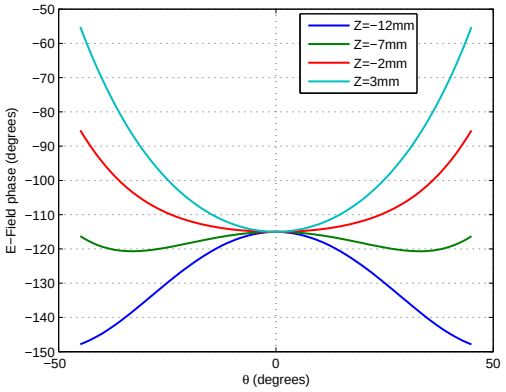

(a)

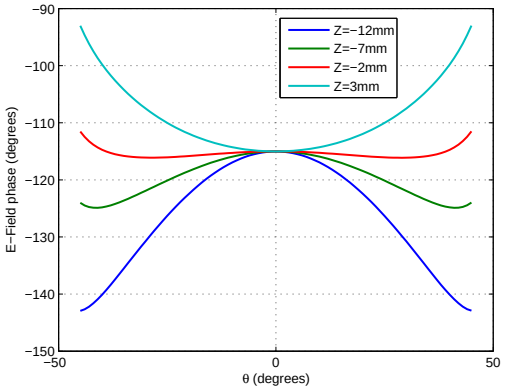

(b)

Fig. 3. Low directive antenna: E-field phase simulations. (a) X-Axis. (b) Y-Axis.

TABLE I
Low directivity antenna @18 GHz X-Axis

Dist.(mm)	n	A	x_0 (mm)	z_0 (mm)	PhC (mm)
170	10	0.9794	2.38e-4	172.0	-2.0
270	16	0.9906	2.11e-4	272.0	-2.0
370	22	0.9946	2.05e-4	372.0	-2.0
470	28	0.9965	2.02e-4	472.0	-2.0
570	34	0.9976	2.00e-4	572.1	-2.1
670	40	0.9983	1.99e-4	672.1	-2.1

B. Directive antenna

The second antenna that has been simulated is another pyramidal horn (WR-42, $H = 70$ mm, $W = 48$ mm, $D = 60$ mm) working at 18 GHz, but with a higher value of directivity (18 dBi). Directive antennas are typically bigger and, therefore, the measurements have to be carried out at a farther distance from the aperture in order to avoid the reactive zone of the NF.

In Figs. 4(a) and 4(b), the results of the estimation of the PhC position are depicted for both the X- and Y-Axis. It can be observed that the PhC position is approximately the same ($Z = -47\ mm$) for both principal planes.

In Table III, the results of the PhC position in the X-Axis

TABLE II
LOW DIRECTIVITY ANTENNA @18 GHZ Y-AXIS

Dist. (mm)	n	A	y_0 (mm)	z_0 (mm)	PhC (mm)
170	10	0.9969	2.16e-4	172.0	-2.0
270	16	1.0010	-6.76e-5	272.0	-2.0
370	22	1.0019	-1.72e-4	372.0	-2.0
470	28	1.0021	-2.19e-4	472.0	-2.0
570	34	1.0022	-2.42e-4	572.1	-2.1
670	40	1.0022	-2.56e-4	672.1	-2.1

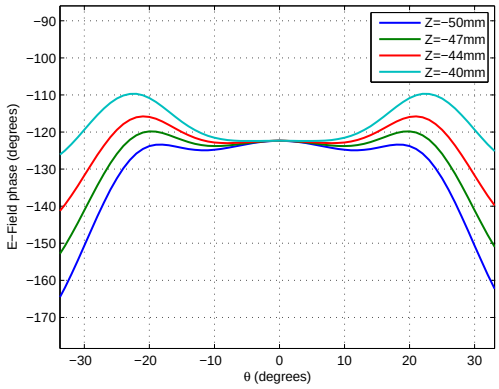

(a)

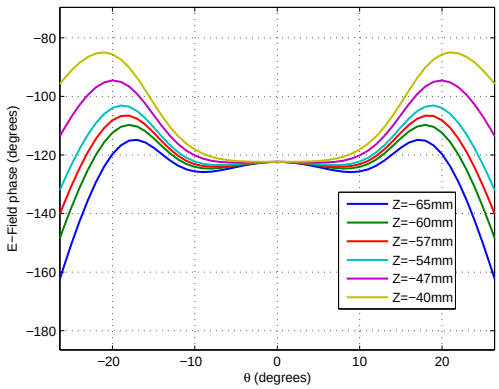

(b)

Fig. 4. Directive antenna: E-field phase simulations. (a) X-Axis. (b) Y-Axis.

are shown. It can be observed that the performance of the method is satisfactory for a wide range of cases, particularly, for distances between 225 mm and 425 mm, by acquiring the field between -90 and 90 mm. When the data are acquired at a farther distance from the antenna aperture, the results of the model can be improved by enlarging the span of the measurement, as it can be seen when the distance is 525mm. Nonetheless, given the results of the model, the PhC position has been accurately estimated in the majority of the cases.

The results for the PhC position given by the method in the Y-Axis (E-Plane) are depicted in Table IV. In this case, these results present a better agreement at a farther distance from the antenna aperture, as long as the initial span is kept. This is due to the existence of secondary lobes in this principal plane

TABLE III
DIRECTIVE ANTENNA @18 GHZ X-AXIS

Dist.(Span) (mm)	n	A	x_0 (mm)	z_0 (mm)	PhC (mm)
225 (-90:90)	16	0.9791	2.52e-4	272.5	**-47.5**
325 (-90:90)	22	1.0059	2.77e-4	372.4	**-47.4**
425 (-90:90)	28	1.0171	2.78e-4	472.3	**-47.3**
525 (-150:150)	34	1.0118	-4.15e-4	572.3	**-47.3**
525 (-90:90)	33	0.9907	2.65e-4	555.6	-30.6
625 (-90:90)	39	0.9954	2.61e-4	655.6	-30.6

TABLE IV
DIRECTIVE ANTENNA @18 GHZ Y-AXIS

Dist.(Span) (mm)	n	A	y_0 (mm)	z_0 (mm)	PhC (mm)
225(-90:90)	18	0.9980	8.82e-5	305.9	-80.9
225(-70:70)	18	1.0083	1.00e-4	305.9	-80.9
325(-90:90)	23	1.0027	8.81e-5	389.1	-64.1
325(-70:70)	22	0.9810	8.11e-5	372.4	**-47.4**
425(-90:90)	28	0.9959	7.65e-5	472.3	**-47.3**
525(-90:90)	34	1.0084	7.08e-5	572.3	**-47.3**
625(-90:90)	40	1.0128	6.75e-5	672.3	**-47.3**

of the antenna, whose effect diminishes when the distance increases or the span of the measurement decreases. In the case that the points at which the field is acquired are closer to the AUT, the effect of the secondary lobes is the greatest in the extremes of the measurement. In Fig. 5 the amplitude for the closer cases is depicted, showing this phenomenon that distorts the results obtained with the method. It can be appreciated a at the sides of the measurement when the distance from the antenna is 225 mm. It also happens for the 325 mm case, but it is not so significant as in the previous case and therefore, it is not distinguishable in the figure. In Table IV it can be seen that the result for the 225mm distance is not improved when the span of the measurement is decreased, where it does improve for the 325mm distance case.

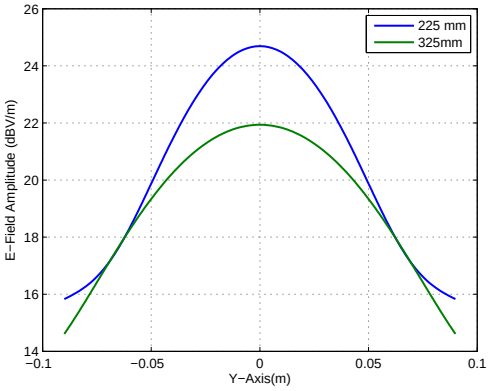

Fig. 5. Comparison of the field amplitude for different simulations.

C. Highly directive antenna

The last AUT simulated is a pyramidal horn (WR-42, $H = 384$ mm, $W = 76$ mm, $D = 102$ mm) presenting a very high directivity (28dBi). Consequently, in this example the effects of the the secondary lobes are going to be greater and the measurements will have to be carried out in a larger span and at a slightly farther distance from the aperture. Figs. 6(a) and 6(b) show the estimation of the PhC position for both axes. It can be observed that these values are slightly different, that is, $Z = -152\ mm$ for X-Axis and $Z = -136\ mm$ for the Y-Axis.

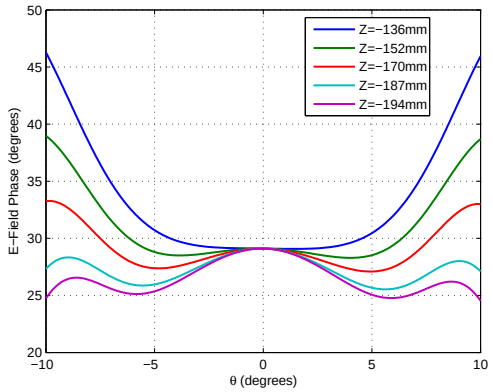

(a)

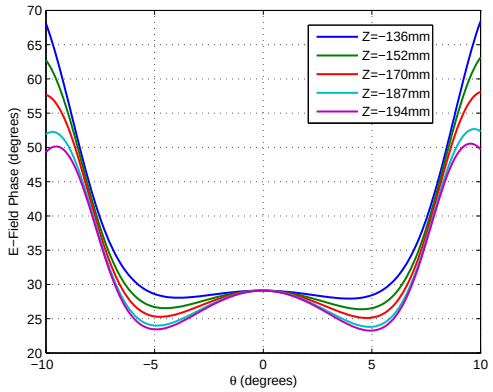

(b)

Fig. 6. Highly directive antenna: E-field phase simulations. (a) X-Axis. (b) Y-Axis.

TABLE V
HIGHLY DIRECTIVE ANTENNA @18 GHZ X-AXIS SPAN -180:180 MM

Dist. (mm)	n	A	x_0 (mm)	z_0 (mm)	PhC (mm)
261	24	1.0031	-7.56e-3	396.7	-135.7
311	28	1.0126	-6.66e-3	463.5	**-152.5**
361	31	0.9997	-3.94e-3	513.5	**-152.5**
411	34	1.0020	6.97e-4	563.5	**-152.5**
461	37	0.9989	8.31e-3	613.5	**-152.5**
511	40	0.9914	1.73e-2	663.5	**-152.5**
561	44	1.0094	2.74e-2	730.2	**-152.5**

TABLE VI
HIGHLY DIRECTIVE ANTENNA @18 GHZ Y-AXIS SPAN -240:240 MM

Dist. (mm)	n	A	y_0 (mm)	z_0 (mm)	PhC (mm)
261	21	0.9960	-6.08e-3	345.1	-84.1
311	25	1.0018	-1.67e-2	412.2	-101.2
361	29	0.9929	-2.15e-2	479.4	-118.4
411	33	1.0002	-2.42e-2	546.3	**-135.3**
461	36	0.9997	-2.49e-2	596.3	**-135.3**
511	39	1.0033	-2.25e-2	646.3	**-135.3**
561	42	0.9884	-2.52e-2	696.3	**-135.3**

In Tables V and VI it can be seen that the results of the method present a good concordance with the expected results when the measurements are carried out at the farthest distances from the antenna aperture. In this case, it has to be taken into account that this feature requires that the data must be acquired in a wider span.

D. Displaced case

Finally, in order to complete the validation process of the proposed method throughout simulations, the low directive AUT has been used to prove the functioning of the system in the case that the measurement path lies on a plane $y = y_0$, which is equivalent to the measurement system not being centered in the antenna aperture. In this case, the phase of the electric field is measured at two different distances (270 mm and 370 mm) from the antenna aperture, being both of them separated 40mm (y_0) from the plane $y = 0$.

TABLE VII
DISPLACED CASE SPAN -90:90 MM

Dist. (mm)	n	A	x_0 (mm)	C
270	16	0.9910	6.54e-4	0.0756 (C_1)
370	22	0.9947	4.94e-4	0.1400 (C_2)

Table VII shows the results of applying the method to the two set of measurements. By using eqs. (10) and (11), it is obtained that $PhC = -2.1$ mm and $y_0 = 39.3$ mm. Then, it can be seen that the results of the method show a good agreement with the expected ones. This validates the functioning of the model when the data are not acquired along the main cuts of the antenna.

IV. MEASUREMENTS

Once the method has been validated through simulations, the next step is to use it to study the PhC of real measured antennas in a planar range [8] in order to be able to characterize them. This way, three different antennas have been analyzed: a corrugated horn, a pyramidal horn and a quasi-yagi antenna, shown in Figs. 7 and 8.

A. Corrugated horn

The first AUT is a corrugated horn working at the frequency of 10GHz (X-Band) with a directivity of 13dBi. In order

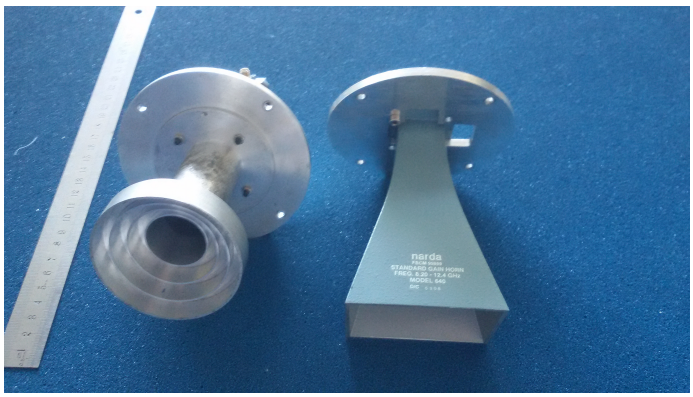

Fig. 7. Photograph of the measured antennas: corrugated an pyramidal horn.

to be able to estimate the position of the PhC, the field of the antenna has been acquired between -100 and 100 mm at several distances from the aperture of the horn. The application of the model for several measurements serves as a form of double-checking the performance of the method.

TABLE VIII
CORRUGATED HORN ANTENNA @10 GHZ X-AXIS SPAN -100:100 MM

Dist. (mm)	n	A	x_0 (mm)	z_0 (mm)	PhC (mm)
72	4	1.1067	-6.65e-1	112.8	-40.8
122	5	1.0583	-4.29e-1	162.6	-40.6
172	7	1.0531	-1.40e-1	212.5	-40.5
222	9	1.0475	-4.55e-2	262.2	-40.2

TABLE IX
CORRUGATED HORN ANTENNA @10 GHZ Y-AXIS SPAN -100:100 MM

Dist. (mm)	n	A	y_0 (mm)	z_0 (mm)	PhC (mm)
72	4	1.0667	5.84e-1	112.9	-40.9
122	5	1.0353	4.47e-1	162.7	-40.7
172	7	1.0337	3.64e-1	212.5	-40.5
222	9	1.0427	3.49e-1	262.3	-40.3

Tables VIII and IX include the obtained results, showing that the estimation of the PhC does not depend on the distance at which the data are acquired. Therefore, it may serve as a further validation for the results of the model. In addition, as it was expected from the symmetrical structure of the AUT, the position of PhC is approximately the same for both principal planes.

In this case, since there is no positioning system for the AUT, the measurements have been carried without ensuring that the antenna was centered, that is, y_0 could be different from zero. Thus, for the X-Axis measurements, the analysis of the displaced case is used in order to estimate the relative position with the measurement system.

In Tables X and XI, the results of applying the displaced case of the model to two different sets of measurements are shown. Thus, by using eqs. (10) and (11), the position of the PhC is found to be at 40 mm from the antenna aperture and the values of y_0 are 13.7 and 13.5 mm respectively. This shows that the displacements of the measurement is approximately the same for both cases. Hence, the model could also be used as a form of checking the alignment of the system.

TABLE X
DISPLACED CASE CORRUGATED HORN: MEASUREMENT 1.

Dist.(mm)	n	A	x_0 (mm)	C
122	5	1.0583	-4.29e-1	0.0264 (C_1)
222	9	1.0475	-4.55e-2	0.0688 (C_2)

TABLE XI
DISPLACED CASE CORRUGATED HORN: MEASUREMENT 2.

Dist. (mm)	n	A	x_0 (mm)	C
172	5	1.0583	-1.40e-1	0.0451 (C_1)
222	9	1.0475	-4.55e-2	0.0688 (C_2)

B. Pyramidal horn

The second AUT is a pyramidal horn working at 10GHz, that presents a slightly higher directivity (16dBi), enabling to make a further validation of the system with a more directive antenna. This way, by applying the method to the acquired data, the PhC position is obtained. This feature is shown in Tables XII and XIII, where it can be seen that its value does not depend significantly on the distance at which the measurement took place. Thus, it can be inferred that the method has accurately estimated the position of the PhC position.

TABLE XII
PYRAMIDAL HORN ANTENNA @10 GHZ X-AXIS SPAN -100:100 MM

Dist. (mm)	n	A	x_0 (mm)	z_0 (mm)	PhC (mm)
60	3	1.0647	1.0	102.9	-42.9
110	5	0.9212	1.89e-1	153.5	-43.5
160	7	0.9876	7.11e-1	203.0	-43.0
210	8	1.0391	-1.04e-1	252.6	-42.6

TABLE XIII
PYRAMIDAL HORN ANTENNA @10 GHZ Y-AXIS SPAN -100:100 MM

Dist. (mm)	n	A	y_0 (mm)	z_0 (mm)	PhC (mm)
60	3	1.0255	-5.26e-1	103.2	-43.5
110	5	0.9696	-7.95e-2	153.3	-43.3
160	7	1.0050	-9.17e-2	202.8	-42.8
210	8	1.0525	-9.41e-2	252.3	-42.3

C. Quasi-yagui antenna

Finally, a quasi-yagi antenna working in X-Band has been analyzed at the frequency of 10GHz. Since this antenna is intended to be used as the feeder element for a transmitarray lens [9], it is very important to determine its PhC position, as

it should be placed at the focus of the structure in order to maximize the directivity of the whole antenna.

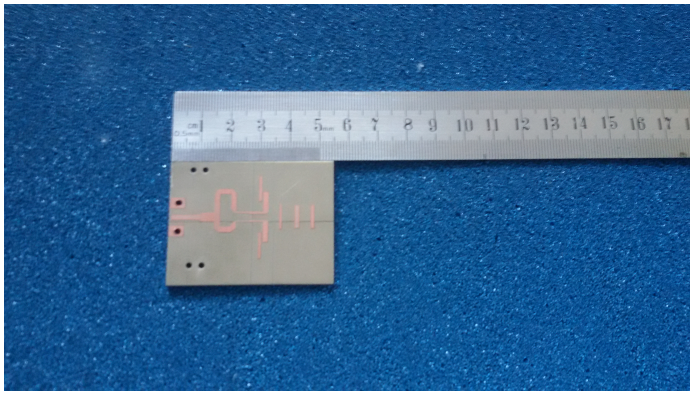

Fig. 8. Photograph of the measured quasi-yagi antenna.

TABLE XIV
QUASI-YAGI ANTENNA @10 GHZ X-AXIS

Dist. (mm)	n	A	x_0 (mm)	z_0 (mm)	PhC (mm)
95	4	0.9682	7.89e-1	128.1	-33.1
145	6	1.0088	9.54e-1	177.8	-32.7
195	8	1.0216	9.40e-1	227.6	-32.6
245	8	1.0198	1.0	277.6	-32.6

TABLE XV
QUASI-YAGI ANTENNA @10 GHZ Y-AXIS

Dist. (mm)	n	A	y_0 (mm)	z_0 (mm)	PhC (mm)
95	4	1.0486	7.02e-3	127.8	-32.8
145	6	1.0547	3.75e-3	177.5	-32.5
195	8	1.0512	-9.26e-2	227.4	-32.4
245	8	1.0485	-2.91e-1	277.4	-32.4

The results of this study are shown in Tables XIV and XV, making clear that the PhC position is at approximately 32 mm from the upper side of the antenna for both principal planes. Moreover, by analyzing the values of the parameter x_0, it can be seen that itis slightly higher for the E-Plane due to the effect of the balun, which introduces a displacement in the position of the PhC.

V. CONCLUSIONS

In this paper, a simple experimental method to estimate the position of the PhC of an antenna has been presented. The method is based on linear planar measurements and it has been validated against simulations, showing good agreement between the estimated position and the one observed from simulations. Afterwards the method has been satisfactorily applied to find the PhC position of different antennas through measurements carried out in a planar range. It has been observed that the major concern of the method is with the estimation of the PhC of highly directive antennas, since the effect of the secondary lobes, which are more frequent in these cases, can alter the final results. Nevertheless, this can be overcome by leaving them out of the data, that is, using a shorter span in the measurement while still using a sufficient number of points, or by acquiring the data at a farther distance from the AUT. Then, according to its working principle, this model would allow to complete the characterization of any antenna, regardless of its structure. Finally, since the calculations of the method are simple, it could also be applied in situ on real-time and thus making it possible to use it as a simple antenna alignment system.

ACKNOWLEDGMENT

The present work has been developed under the support of the FPI pre-doctoral grant with ref no. BES-2012-053154, the project MIRIIEM with ref. TEC2014-540005-P of the Ministerio de Economía y Competitividad, and the research project of the Gobierno del Principado de Asturias / FEDER with ref. GRUPIN14-114.

REFERENCES

[1] J. Huang and J.A. Encinar, *Reflectarray antennas*, IEEE Press, 2008.
[2] D. M. Pozar, *Flat lens antenna concept using aperture coupled microstrip lpatches*, Electronic Letters, vol. 32, pp. 2109-2111, 1966.
[3] P. Padilla, P. Pousi, A. Tamminen, J. Mallat, J. Ala-Laurinaho, M. Sierra-Castaner and A. V. Räisänen, *Experimental determination of DRW antenna phase center at mm-wavelengths using a planar scanner: comparison of different methods*, IEEE Transactions on Antennas and Propagation, vol. 59, no. 8, pp. 1481-1487, Aug. 2011.
[4] Z. Y. Hu, Z. Li, O. Gang and Z. Bin, *Research on antenna phase center anechoic chamber calibration method*, 2010 International Conference on Microwave and Millimeter Wave Technology (ICMMT), pp. 1522 - 1524, 2010.
[5] E. I. Muehldorf, *The phase center of horn antennas*, IEEE Transactions on Antennas and Propagation, vol. 18, no.6 , pp. 753-760, Nov. 1970.
[6] J. R. Costa, E. B. Lima and C. A. Fernandes, *Antenna phase center determination from amplitude measurements using a focusing lens*, 2010 IEEE Antennas and Propagation Society International Symposium, 2010.
[7] FEKO 6.2. https://www.feko.info/about-us/News/release-of-feko-suite-6.2-feature-overview
[8] A. Arboleya, Y. Álvarez and F. Las-Heras, *Millimeter and sub-millimeter planar measurement setup* , 2013 IEEE Antennas and Propagation Society International Symposium, Orlando(FL), 2013.
[9] E. G. Plaza, J. R. Costa, C. A. Fernandes, G. León, S. Loredo and F. Las-Heras, *A multibeam antenna for imaging based on planar lenses* , The 9th European Conference on Antennas and Propagation (EuCAP), Lisbon, 2015.